PROCEEDINGS OF SPIE

SPIEDigitalLibrary.org/conference-proceedings-of-spie

Modeling mode-locked Bismuth laser for soliton generation in the normal and anomalous dispersion regime

Zajnulina, M., Korobko, D., Shchukarev, Igor, Fotiadi, A.

M. Zajnulina, D. A. Korobko, Igor Shchukarev, A. A. Fotiadi, "Modeling mode-locked Bismuth laser for soliton generation in the normal and anomalous dispersion regime," Proc. SPIE 11357, Fiber Lasers and Glass Photonics: Materials through Applications II, 113570J (1 April 2020); doi: 10.1117/12.2557687

SPIE.

Event: SPIE Photonics Europe, 2020, Online Only, France

Modeling Mode-Locked Bismuth Laser for Soliton Generation in the Normal and Anomalous Dispersion Regime

M. Zajnulina[*a], D. A. Korobko[b], Igor Shchukarev[b], A. A. Fotiadi[b,c]
[a]Aston Institute of Photonic Technologies, Aston University, B4 7ET Birmingham, United Kingdom; [b]Ulyanovsk State University, 42 Leo Tolstoy Street, Ulyanovsk, 432970, Russian Federation; [c]University of Mons, blvd. Dolez 31, Mons, B-7000, Belgium

ABSTRACT

A scheme of a passively mode-locked fiber laser that deploys a Bismuth-doped germano-phosphosilicate fiber as an active medium is introduced. It operates at Bismuth amplification maximum of 1320 nm if suitably pumped at 1220 nm. We also introduce a model to describe the nonlinear light propagation in this laser in the regime of normal and anomalous group-velocity dispersion. The model is developed for two polarizations states accounting for a broad range of dynamical regimes connected to the state of cavity polarization. It also includes a low level of amplification in Bismuth. Depending on the level of the gain saturation energy, we observe the formation of stable dissipative solitons or incoherent pulses in the normal cavity group-velocity dispersion regime or the formation of single or two solitons per roundtrip in the anomalous dispersion regime. The results coincide well with already published experimental observations of dynamics in Bismuth lasers at 1320 nm which validates our model. As for the application potential, the introduced laser scheme can be used to effectively treat skin acne and various other medical applications.

Keywords: bismuth laser, mode-locked fiber lasers, dissipative solitons, optical solitons, lasers for medical application

1. INTRODUCTION

Mode-locked fiber lasers are robust and low-cost lasers for generation of ultrashort optical pulses. Picosecond- and sub-picosecond-lasers specifically in the near-IR range around 1300 nm have a great application potential in various fields of science and technology such as telecommunication or material processing [1]. Specifically in the field of medical application, it was reported that laser illumination at 1320 nm can help to reduce acne [2], whereas laser light at 1300 nm can be used to close wounds [3]. Laser wavelengths in the range of $1265 - 1270$ nm correspond to the maximum of the oxygen absorption band. Access and excitation of this (singlet) oxygen has a variety of further medical applications. Thus, laser light at 1270 nm has an anti-inflammatory effect on the tissue [4]. Light at 1268 nm helps to kill cancer cells [5]. Laser light at 1265 nm can be used to modulate the vital characteristics of in-vitro and in-vivo cells [6]–[8]. Previously, solid state (Nd:YAG [2], [3]) or InGaAs / InAs quantum dot laser diodes ([5]) were used for this kind of applications due to the lack of fiber-based counterparts which was due to the absence of suitable fiber amplifiers in this spectral range. The introduction of Bismuth- (Bi-) doped fibers gave birth to the possibility to access NIR spectral ranges that were not reachable by fiber lasers that deploy such established amplifying media as Erbium, Ytterbium, and Thorium [1], [9], [10]. Various host glasses for Bi-dopants and the specifically skewed amplification profile of Bismuth in germano-phosphosilicate fiber allow to access the spectral range at specifically $1265 - 1320$ nm opening a window of possibilities for development of fiber lasers for medical applications [11]–[13].

Although highly promising, Bi is considered to be a challenging and not yet fully understood amplifying medium (cf. [1]). Thus, one of the limitations of Bi-doped fibers is a quite low level of amplification if compared with Erbium- or / and Ytterbium-doped counterparts. To overcome this specific, longer and, thus, more nonlinear and noisy cavities are required. Careful studies, both of experimental and theoretical / numerical nature, are needed to develop Bi-lasers specifically for medical application where the easiness and long-term operation stability are decisive. Several experimental studies were reported on successful realization of various types of fiber Bi-lasers and amplifiers [14]–[19]. Exhaustive theoretical and numerical consideration of the pulse generation and evolution are – to our best knowledge – still missing. To encounter

[*]m.zajnulina@aston.ac.uk; phone +44 (0)121 204 5070

Fiber Lasers and Glass Photonics: Materials through Applications II, edited by Maurizio Ferrari, Jacob I. Mackenzie, Stefano Taccheo, Proc. of SPIE Vol. 11357, 113570J · © 2020 SPIE
CCC code: 0277-786X/20/$21 · doi: 10.1117/12.2557687

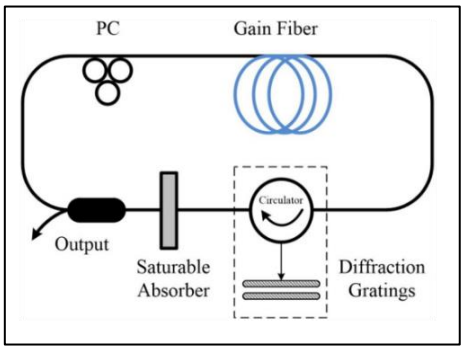

Figure 1. The scheme of a ring mode-locked fiber laser where the Gain Fiber is a Bismuth-doped fiber and a diffraction grating is used to change the group-velocity dispersion from normal to anomalous regime. PC is the polarization controller. Output is the output coupler.

this problem, we introduce a scheme of a ring fiber laser that deploys a Bi-doped germano-phosphosilicate fiber as amplifying medium (cf. [13], [17]). It is passively mode-locked by a saturable absorber. We also introduce a dynamical model for the nonlinear light propagation in this laser and study the pulse generation and evolution at Bi amplification maximum of 1320 nm in the range of normal and anomalous group-velocity dispersion (GVD). In particular, we focus our attention on the possibility of the regime tuning from dissipative solitons in the normal GVD regime to optical solitons that arise in the anomalous GVD range. To do so, we include Bi-specific features in consideration such as i) low value of normal GVD close to 1320 nm, ii) the according possibility of a regime change from normal to anomalous GVD if an additional GVD compensator is applied, and iii) low-level amplification that implies the usage of long Bi-doped fibers leading to a high-level nonlinearity in the laser cavity.

Tuning the laser pump level (that is represented by the gain saturation energy in the studies below), we are able to determine the energy region of a stable dissipative soliton generation, the region of instability, and the region of a noisy pulse generation in the normal GVD regime. When the net GVD of the cavity becomes anomalous under the impact of a pair of diffraction gratings, we observe the generation of single and two optical solitons in the cavity depending on the value of gain saturation energy. Our numerical results coincide well with the reported experimental observations (cf. [13], [17], [20]).

2. LASER SCHEME AND THE MATHEMATICAL MODEL

2.1 Tunable Bismuth Fiber Laser

The scheme of a passively mode-locked fiber ring laser deploying Bi as amplifying medium is shown in Fig. 1. This laser uses a saturable absorber for mode-locking and a diffraction grating to change the GVD from normal to anomalous regime. We use a germano-phosphosilicate fiber doped with Bi as the Gain Fiber (Fig. 1). If pumped at 1.22 μm, this fiber has an amplification maximum at $\lambda_0 = 1320$ nm [17]. Without the influence of the diffraction gratings, the net cavity dispersion is slightly positive, but close to zero. This allows for a change of the laser operation regime towards the generation of ultra-short optical soliton pulses (living in the anomalous dispersion regime) if a pair of diffraction gratings is used.

2.2 Mathematical Model

In the modelling of the introduced laser scheme, the Bi-doped gain fiber is considered to be the only distributed, i.e. extended, part of the cavity where the light propagation depends on the time variable t and the propagation variable z. Any other parts of the laser such as the polarization controller, saturable absorber, output coupler, and the diffraction gratings are considered to be lumped, i.e. localized, elements with instantaneous action. The model we use for the nonlinear propagation of light in the Bi-doped amplifying fiber consists of a system of coupled Ginzburg-Landau Equations for complex fields of two polarization states denoted by X and Y ([21], [22], [23], cf. [24]).

$$\frac{\partial A_X}{\partial z} - i\frac{\beta_2}{2}\frac{\partial^2 A_X}{\partial t^2} + \frac{\beta_3}{6}\frac{\partial^3 A_X}{\partial t^3} - i\gamma\left(|A_X|^2 + \frac{2}{3}|A_Y|^2\right)A_X - \frac{i}{3}\gamma A_X^* A_Y^2 = \frac{g}{2}A_X + \frac{\beta_{2f}}{2}\frac{\partial^2 A_X}{\partial t^2} \qquad (1)$$

$$\frac{\partial A_Y}{\partial z} - i\frac{\beta_2}{2}\frac{\partial^2 A_Y}{\partial t^2} + \frac{\beta_3}{6}\frac{\partial^3 A_Y}{\partial t^3} - i\gamma\left(|A_Y|^2 + \frac{2}{3}|A_X|^2\right)A_Y - \frac{i}{3}\gamma A_Y^* A_X^2 = \frac{g}{2}A_Y + \frac{\beta_{2f}}{2}\frac{\partial^2 A_Y}{\partial t^2}$$

The consideration of both polarization states allows for studying of a broad range of dynamical regimes in a fiber mode-locked laser (cf. [25]–[28]). In Eqs. 1, β_2 is the GVD parameter, whereas β_3 describes the third-order dispersion (TOD) that is particularly important to be considered when GVD values are close to 0 (which is the case here). γ is the Kerr nonlinearity coefficient that is responsible for self-phase and cross-phase modulation. The initial condition for Eqs. 1 is described by a low-amplitude Gaussian noise that is equally distributed between both polarization states, i.e. $A_{X0} = A_{Y0}$.

The difference between Eqs. 1 and a set of standard Nonlinear Schrödinger Equations for nonlinear light propagation in optical fibers consists in the contribution of an additional dispersive term (the last terms on the right side in Eqs. 1). Here, the parameter

$$\beta_{2f} = \frac{g}{\Omega_g^2} \qquad (2)$$

describes the parabolic shape of the gain g with Ω_g^2 that determines the amplification linewidth at FWHM in s^{-1}. The maximum of the amplifying spectrum parabola lies at $\lambda_0 = 1320\ nm$ [17]. Further, we assume a gain that saturates as the optical pulses propagate along the Bi-doped fiber [21]:

$$g(z,t) = g(z) = g_0 \left(1 + \frac{\int_0^{\tau_{win}} \left(|A_X(z,t)|^2 + |A_Y(z,t)|^2\right) dt}{E_g}\right)^{-1} \qquad (3)$$

where g_0 is the small-signal gain coefficient, E_g the gain saturation energy, and $\tau_{win}$the temporal window of our modelling.

The action of the lumped cavity elements such as the polarization controller, saturable absorber, the output coupler, and the pair of diffraction gratings is described by suitable transfer functions (cf. [29]). Thus, the polarization controller with a certain angle θ changes the amplitude of the polarization states such as $A_i' = A_i \exp(i\theta)$, $i \in \{X, Y\}$. Further, we assume the saturable absorber to be instantaneous and express its action via the transfer function $A_i' = (1 - \alpha)A_i$ with the saturated loss coefficient

$$\alpha = \frac{\alpha_0}{1 + (|A_X(z,t)|^2 + |A_Y(z,t)|^2)/P_s} \qquad (4)$$

where $\alpha_0$is the unsaturated loss and P_s is the saturation power of the absorber. The losses due to the output coupler that diverges 10% of the light power out of the cavity are modelled by the transfer function $A_i' = \sqrt{0.9}A_i$. The transfer function for the diffraction gratings is given by $A_i' = A_i \beta_{2dif} \omega^2/2$ with β_{2dif} being the GVD parameter of the gratings.

The numerical integration of Eqs. 1 as well as the subsequent application of the lumped element transfer functions was done by means of the standard SSF (split-step Fourier) method in a time window of 164 ps sampled with 2^{13} points. The cavity output data was collected after 500 cavity roundtrips. The numerical parameters chosen for the simulations are listed in Tab. 1. They are close to Bi-laser parameters taken or measured in a real experiment [12], [17], [11].

Table 1. Cavity parameters used for numerical simulation of nonlinear light propagation in a passively mode-locked Bismuth fiber laser.

Parameter	Value
Nonlinear coefficient $\gamma\ [W^{-1}km^{-1}]$	2
Group-velocity dispersion GVD $\beta_2\ \left[\frac{ps^2}{km}\right]$	2.5
Third-order dispersion $\beta_3\ \left[\frac{ps^3}{km}\right]$	0.02
Small-signal gain $g_0\ [m^{-1}]$	0.02
FWHM of the Bismuth amplifying line $\sqrt{2}\ \Omega_g\ [ps^{-1}]$	47.1 $(\sim 45\ nm\ @\ \lambda_0 = 1320\ nm)$
Bi-doped fiber length $L_g\ [m]$	30
Unsaturated loss of the saturable absorber α_0	0.25
Saturation power $P_s\ [W]$	30
Diffraction grating GVD $\beta_{2dif}\ [ps^2]$	$-0.2 \ldots -0.6$
Polarization controller angle θ	$3\pi/8$

3. RESULTS

Let us first put the diffraction gratings aside and consider the generation of optical pulses out of the initial Gaussian noise in the normal GVD regime of the laser operation at $\lambda_0 = 1320$ nm. In particular, we first consider the generation of optical

pulses as a function of the gain saturation energy E_g that can be seen as the level of the laser pump energy. The net cavity dispersion is positive, but close to zero in this case, i.e. $\beta_{2\mathrm{NET}} = 0.075\ \mathrm{ps}^2$. Some results of this numerical experiment are shown in Fig. 2.

In the range from $E_g = 100$ pJ to around $E_g = 210$ pJ, the whole cavity energy is accumulated in one well-shaped and stable mode-locked dissipative soliton with a temporal width of around 10 ps (Fig 2.b) [30], [31], [32]. As expected, the pulse energy as well as the pulse spectral width increase with the value of E_g (Fig. 2.a and Fig. 3.a). At small values of GVD, the pulse gains unstable frequency modulation and eventually breaks when the spectral width of the pulse becomes larger and larger due to the increase of energy [33]. Due to this break-up mechanism, the generation of high-energy pulses is prevented in the range of $E_g > 210$ pJ and $E_g = 280$ pJ. (Fig. 2.a). If the red flank of the pulse spectrum penetrates the spectral range of the anomalous GVD due to the further increase of E_g, the dissipative soliton becomes unstable and explodes into a series of several sub-pulses that all together build up a noisy, incoherent optical pulse (Figs. 2.c and 3.a, $E_g = 350$ pJ) (cf. [34]).

A pair of diffraction gratings with $\beta_{2dif} = -0.2\ \mathrm{ps}^2$ is now used to change the net cavity dispersion from the initial value of normal GVD with $\beta_{2NET} = 0.075\ \mathrm{ps}^2$ to the anomalous GVD with $\beta_{2NET} = -0.125\ \mathrm{ps}^2$ (cf. Fig. 1) and to study the impact of the grating GVD on the features of the generated pulses (cf. [35]). This leads to a laser regime when ultra-short optical solitons are generated (Fig. 4). Optical solitons in the anomalous GVD range are characterised by a quite low level of pulse energy (which is the result of the soliton energy quantization [36]) and a transition to a multi-pulse generation at lower pumping energies than in the case of normal cavity dispersion [37].

Fig. 4.a shows the cavity energy vs. the gain saturation energy E_g. For $E_g < 35$ pJ, this energy is accumulated in a single optical pulse being an optical soliton (Fig. 4.d) (cf. [36]). For energies $35\ \mathrm{pJ} \leq E_g < 65$ pJ, we observe a transition regime in which the number of pulses is not stable. For $E_g \geq 65$ pJ, the cavity operates in the regime when two (separated) optical solitons are generated due to the soliton energy quantization (Fig. 4.e) [36]. The according pulse spectra have shapes that are typical for pulses generated in mode-locked lasers, namely the shapes of optical solitons with some Kelly-sidebands that arise due to the periodic perturbation of the pulses inside the cavity (cf. Fig. 3.b) [38]. The pulse duration hardly

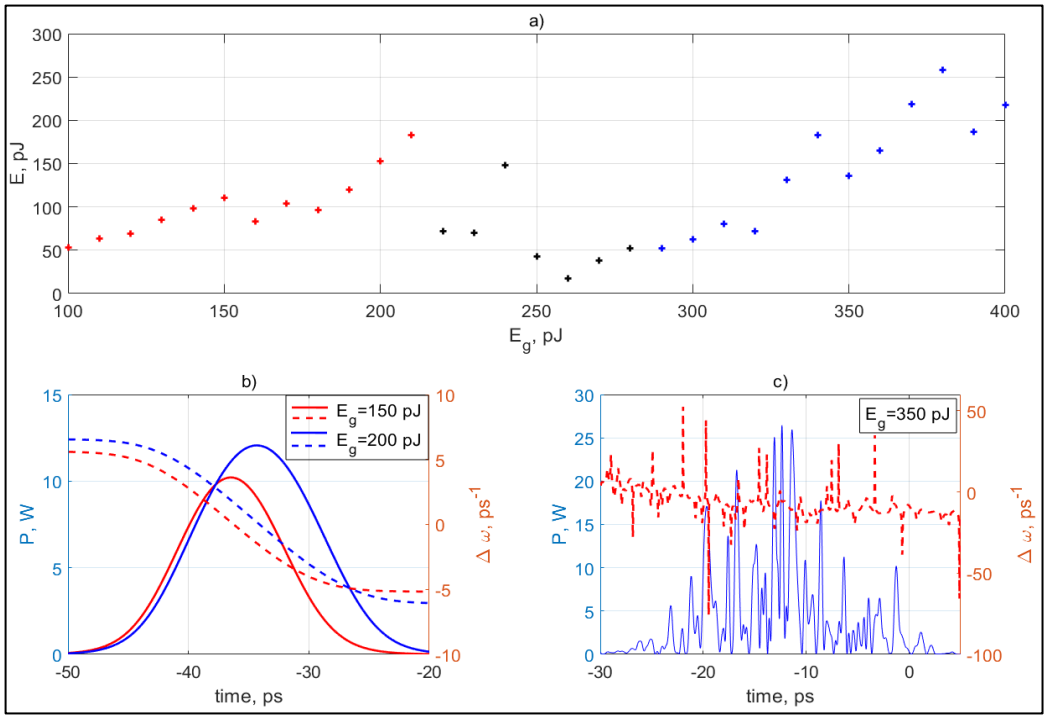

Figure 2. a) Cavity energy accumulated in a single dissipative soliton vs. gain saturation energy E_g in the normal group-velocity dispersion regime. Red crosses denote the range of the dissipative soliton generation, black ones the transition regime, and blue ones the regime of noisy pulses. b) and c) Pulse temporal shapes (only the X-polarization state is shown) and the instantaneous pulse frequency for different values of saturation energy.

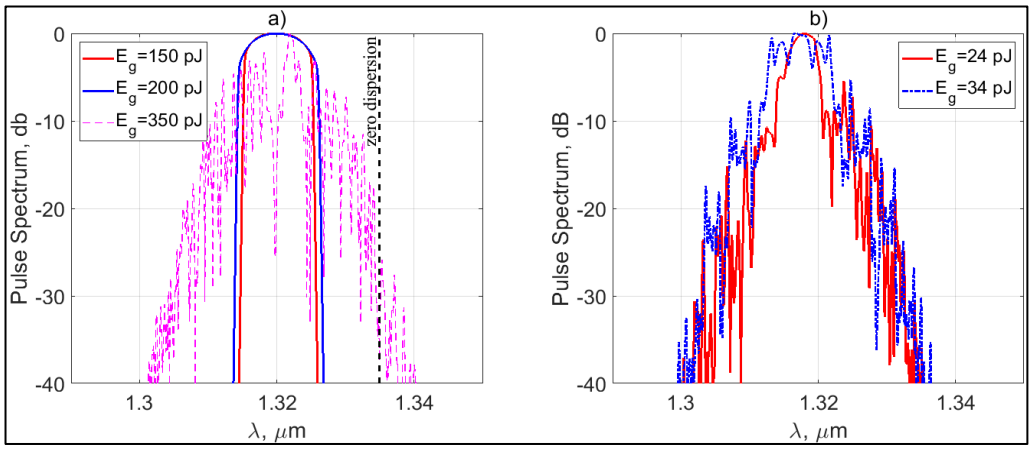

Figure 3. a) Spectra of the generated pulses for different values of the gain saturation energy $E_g$in the normal cavity group-velocity dispersion regime at the amplification maximum of the Bismuth-doped fiber @ $\lambda_0 = 1320\,nm$. b) Spectra obtained after the deployment of a diffraction grating with the group-velocity dispersion of $\beta_{2dif} = -0.2\,ps^2$ to switch to the anomalous cavity dispersion regime.

changes with the value of E_g and is almost equal for both regimes of single and two solitons (Figs. 4.b and 4.c). This is because the duration is mainly determined by the balance between the nonlinearity of the cavity and its GVD value (cf. [39]) contrary to the case of dissipative solitons whose shapes are determined by a delicate balance between the dispersion, nonlinearity, and the energy dissipation. For the chosen value of $\beta_{2dif} = -0.2$ ps^2, the pulse duration is $\tau_{FWHM} \approx 0.8$ ps which coincides with the soliton (sech-profile) pulse width of $\tau_{sech} \approx 0.45$ ps. Fig. 4.d and Fig. 4.e show the typical sech-

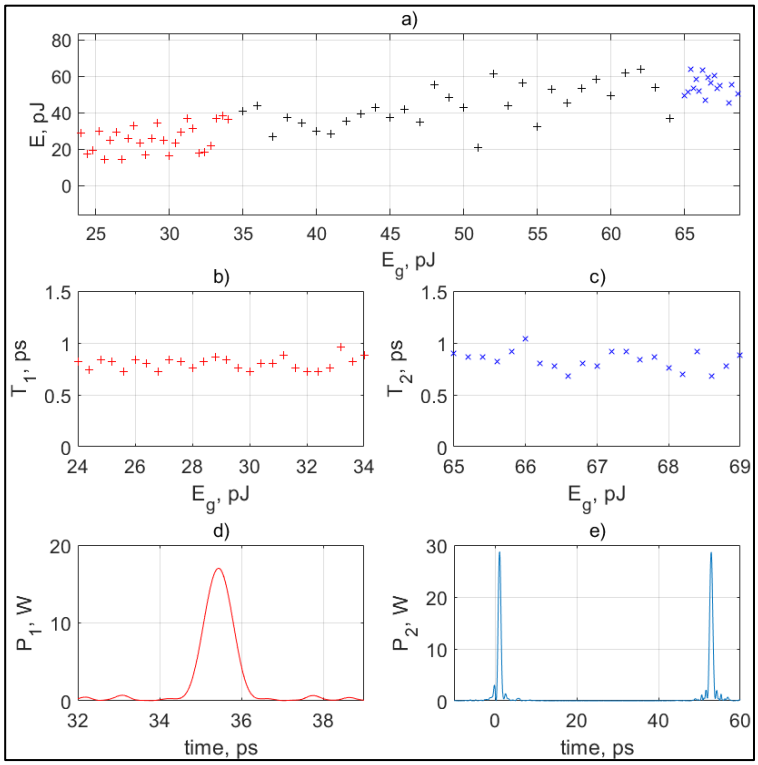

Figure 4. a) Cavity energy vs. gain saturation energy $E_g$in the net anomalous cavity group-velocity dispersion regime with $\beta_{2NET} = -0.125$ ps^2. Red crosses denote the range of a single soliton, black crosses the transition range, and blue ones the range when two solitons are generated. b) and c) Temporal FWHM in the single- (b) and two- (c) soliton regime depending on the level of E_g. d) Temporal shape of a single-soliton generated at $E_g = 28.4$ pJ. e) Temporal shape of a two-soliton generation at $E_g = 67.4$ pJ. Note: only the X-polarization state is depicted.

profiles of the generated pulses with the contribution of the dispersive waves that manifest themselves in pronounced pulse pedestals.

Now, we consider the impact of different values of the grating GVD parameter β_{2dif} on the features of generated solitons. Fig. 5.a shows the cavity energy and Fig. 5.b presents the FWHM pulse width as the functions of the grating GVD parameter for values $-0.2\ \text{ps}^2 \geq \beta_{2dif} \geq -0.6\ \text{ps}^2$. The results are presented for two values of the gain saturation energy E_g giving birth to a single- and two-soliton regime, respectively. Taking into account the dispersive-wave components, we conclude from our observations that the soliton energy only weakly depends on the value of β_{2dif}. At the same time, as expected, the pulse duration increases with the absolute value of β_{2dif} (Fig. 5.b). Thus, soliton profile pulse width is $\tau_{sech} \approx 0.45$ ps at $\beta_{2dif} = -0.2\ \text{ps}^2$ and $\tau_{sech} \approx 0.8$ ps at $\beta_{2dif} = -0.6\ \text{ps}^2$.

4. CONCLUSION AND DISCUSSION

Here, we introduced a scheme of a fiber ring laser that deploys a germano-phosphosilicate fiber doped with Bismuth as an amplifying medium and that is passively mode-locked with a saturable absorber. This laser operates at Bismuth amplification maximum of 1320 nm if suitably pumped at 1220 nm. We also introduce a model to describe the pulse generation in this laser in the regime of normal and anomalous group-velocity dispersion. In this model, we include such specific of Bismuth as the low-level of amplification which requires the usage of long active fibers and, thus, implies a high level of the total nonlinearity in the cavity. We numerically integrate the model to study the pulse generation in the normal and anomalous dispersion regime depending on the level of the gain saturation energy that can be considered as the cavity pump level. The observed numerical results coincide well with the experimental results reported in Ref. [40] and Ref. [20]. Thus, we are convinced that the presented model as well as the model parameters can be used for further studies of the nonlinear light propagation in Bismuth fiber lasers at 1320 nm, the wavelength at which, for instance, acne can be successfully treated [2].

In detail, in the normal dispersion regime, we observe the generation of dissipative solitons whose temporal and spectral width increases with the level of the gain saturation energy. However, this level has an upper limit at which the dissipative solitons start to break due to the fact that the net cavity dispersion value is close to zero. For higher values of the gain saturation energy, we observe the formation of noisy, incoherent pulses that arise due to the dissipative soliton break-up based on the fact that the red flanks of the broadened soliton spectra enter the anomalous dispersion regime of the fiber.

When a pair of diffraction gratings is used, the net cavity dispersion becomes anomalous. In this regime, we observe the formation of single or two optical solitons per roundtrip depending on the value of the gain saturation energy. Here, the laser exhibits typical characteristics of a soliton source, namely the ultrashort temporal pulse and an easy transition from a single- to multi-pulse operation. From the point of view of the application in medicine, the presented laser scheme enables a quick switch from higher-energetic pulses at slow repetition rates in the normal dispersion regime to lower-energetic pulses at higher repetition rates in the anomalous regime which allows to access the tissues at different depths. In our future

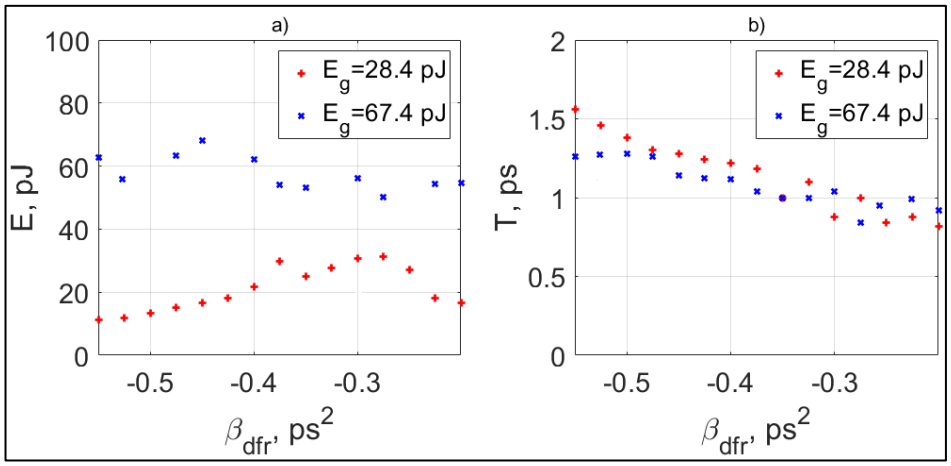

Figure 5. a) Cavity energy and b) the FWHM soliton sech-duration as functions of the group-velocity dispersion parameter of the diffraction gratings for two different values of the saturation energy E_g. $E_g = 28.4\ pJ$ denotes the single-soliton regime, whereas $E_g = 67.4\ pJ$ gives birth to the generation of two solitons.

work, we are planning to investigate the pulse generation of our Bismuth laser at 1300 nm, the wavelength at which wounds can be closed [3], as well as consider the possibility of pulse generation at 1268 nm, the wavelength at which cancer can be successfully treated [5].

5. ACKNOWLEDGEMENTS

D. Korobko acknowledges the funding from the project RSF (project ID: 19-72-10037). A. Fotiadi and I. Shchukarev would like to thank for funding from RFBR (projects ID: 19-42-730009 and 19-42-730013). M. Zajnulina gratefully acknowledges the funding from the H2020-MSCA-IF-2017 scheme (project ID: 792421). We also would like to thank our colleagues E. Manuylovich and I. Kudelin (Aston University Birmingham) for fruitful discussions and contributions.

REFERENCES

[1] E. M. Dianov, "Bismuth-doped optical fibers: a challenging active medium for near-IR lasers and optical amplifiers," *Light Sci. Appl.*, vol. 1, no. e12, May 2012.

[2] J. S. Orringer *et al.*, "A randomized, controlled, split-face clinical trial of 1320-nm Nd:YAG laser therapy in the treatment of acne vulgaris," *J. Am. Acad. Dermatol.*, vol. 56, no. 3, pp. 432–438, Mar. 2007.

[3] D. K. Dew, "Tissue Fusion With 1.3 Micron YAG Laser," in *Proc. SPIE Vol. 1066, p. 34, Laser Surgery: Advanced Characterization, Therapeutics, and Systems, Kazuhiko Atsumi; Norman R. Goldblatt; Stephen N. Joffe; Eds.*, 1989, vol. 1066, p. 34.

[4] D. Dolgova *et al.*, "Anti-inflammatory and cell proliferative effect of the 1270 nm laser irradiation on the BALB/c nude mouse model involves activation of the cell antioxidant system," *Biomed. Opt. Express*, vol. 10, no. 8, p. 4261, 2019.

[5] S. G. Sokolovski, S. A. Zolotovskaya, A. Goltsov, C. Pourreyron, A. P. South, and E. U. Rafailov, "Infrared laser pulse triggers increased singlet oxygen production in tumour cells," *Sci. Rep.*, vol. 3, 2013.

[6] A. Khokhlova *et al.*, "The photobiomodulation of vital parameters of the cancer cell culture by low dose of Near-IR laser irradiation," *IEEE J. Sel. Top. Quantum Electron.*, vol. 25, no. 1, 2019.

[7] A. Khokhlova *et al.*, "The light-oxygen effect in biological cells enhanced by highly localized surface plasmon-polaritons," *Sci. Rep.*, vol. 9:18435, pp. 1–8, 2019.

[8] A. Khokhlova *et al.*, "Effects of high and low level 1265 nm laser irradiation on HCT116 cancer cells," in *SPIE BiOS 2019*, 2019, no. March 2019, p. 21.

[9] K. Murata, Y. Fujimoto, T. Kanabe, H. Fujita, and M. Nakatsuka, "Bi-doped SiO2 as a new laser material for an intense laser," *Fusion Eng. Des.*, vol. 44, pp. 437–439, 1999.

[10] E. M. Dianov, V. V. Dvoyrin, V. M. Mashinsky, A. A. Umnikov, M. V. Yashkov, and A. N. Gur'yanov, "CW bismuth fibre laser," *Kvantovaya Elektron.*, vol. 35, no. 12, pp. 1083–1084, 2005.

[11] I. A. Bufetov *et al.*, "Bi-Doped Optical Fibers and Fiber Lasers," *IEEE J. Sel. Top. Quantum Electron.*, vol. 20, no. 5, pp. 111–125, 2014.

[12] I. A. Bufetov *et al.*, "Efficient bi-doped fiber lasers and amplifiers for the spectral region 1300-1500 nm," *Fiber Lasers VII Technol. Syst. Appl.*, vol. 7580, no. February 2010, p. 758014, 2010.

[13] N. K. Thipparapu, Y. Wang, S. Wang, A. A. Umnikov, P. Barua, and J. K. Sahu, "Bi-doped fiber amplifiers and lasers," *Opt. Mater. Express*, vol. 9, no. 6, p. 2446, 2019.

[14] A. A. Krylov, V. V Dvoirin, V. M. Mashinsky, P. G. Kryukov, O. G. Okhotnikov, and M. Guina, "Mode locking in a bismuth fibre laser by using a SESAM," *Quantum Electron.*, vol. 38, no. 3, pp. 233–238, 2008.

[15] A. A. Krylov, P. G. Kryukov, E. M. Dianov, O. G. Okhotnikov, and M. Guina, "Pulsed bismuth fibre laser with the intracavity-compensated group velocity dispersion," *Quantum Electron.*, vol. 39, no. 1, pp. 21–24, 2009.

[16] I. Razdobreev, L. Bigot, V. Pureur, A. Favre, G. Bouwmans, and M. Douay, "Efficient all-fiber bismuth-doped laser," *Appl. Phys. Lett.*, vol. 90, no. 3, 2007.

[17] R. Gumenyuk, J. Puustinen, A. V. Shubin, I. A. Bufetov, E. M. Dianov, and O. G. Okhotnikov, "1.32 μm Mode-Locked Bismuth-Doped Fiber Laser Operating in Anomalous and Normal Dispersion Regimes," *Opt. Lett.*, vol. 38, no. 20, p. 4005, 2013.

[18] J. Heikkinen *et al.*, "A 1.33 μm picosecond pulse generator based on semiconductor disk mode-locked laser and bismuth fiber amplifie," *Opt. Express*, vol. 22, no. 10, pp. 11446–11455, 2014.

[19] N. K. Thipparapu, C. Guo, A. A. Umnikov, P. Barua, A. Taranta, and J. K. Sahu, "Bismuth-doped all-fiber mode-locked laser operating at 1340 nm," *Opt. Lett.*, vol. 42, no. 24, p. 5102, Dec. 2017.

[20] A. Khegai *et al.*, "Bismuth-doped fiber laser at 132 μm mode-locked by single-walled carbon nanotubes," *Opt. Express*, vol. 26, no. 18, p. 23911, 2018.

[21] D. A. Korobko, A. A. Fotiadi, and I. O. Zolotovskii, "Mode-locking evolution in ring fiber lasers with tunable repetition rate," *Opt. Express*, vol. 25, no. 18, pp. 21180–21190, 2017.

[22] A. S. Abramov, D. A. Korobko, I. O. Zolotovskii, and A. A. Fotiadi, "Spectral compression in ring similariton fiber laser," *Laser Phys. Lett.*, vol. 16, no. 035107, 2019.

[23] J. Rissanen, D. A. Korobko, I. O. Zolotovsky, M. Melkumov, V. F. Khopin, and R. Gumenyuk, "Infiltrated bunch of solitons in Bi-doped frequency-shifted feedback fibre laser operated at 1450 nm," *Sci. Rep.*, vol. 7:44194, pp. 1–10, 2017.

[24] G. P. Agrawal, "Polarization Effects," in *Nonlinear Fiber Optics*, 5th ed., Academic Press, 2012, pp. 193–244.

[25] S. V. Sergeyev, H. Kbashi, N. Tarasov, Y. Loiko, and S. A. Kolpakov, "Vector-Resonance-Multimode Instability," *Phys. Rev. Lett.*, vol. 118, no. 3, pp. 18–22, 2017.

[26] H. J. Kbashi, S. V. Sergeyev, M. Al-Araimi, A. Rozhin, D. Korobko, and A. Fotiadi, "High-frequency vector harmonic mode locking driven by acoustic resonances," *Opt. Lett.*, vol. 44, no. 21, p. 5112, 2019.

[27] H. J. Kbashi, M. Zajnulina, A. G. Martinez, and S. V Sergeyev, "Mulitiscale spatiotemporal structures in mode-locked fiber lasers," *Laser Phys. Lett.*, vol. 17, no. 035103, 2020.

[28] S. Boivinet, J. B. Lecourt, Y. Hernandez, A. A. Fotiadi, M. Wuilpart, and P. Megret, "All-fiber 1-μm PM mode-lock laser delivering picosecond pulses at sub-MHz repetition rate," *IEEE Photonics Technol. Lett.*, vol. 26, no. 22, pp. 2256–2259, 2014.

[29] G. P. Agrawal, *Applications of Nonlinear Fiber Optics*, 2nd ed. Academic Press, 2008.

[30] W. H. Renninger, A. Chong, and F. W. Wise, "Dissipative solitons in normal-dispersion fiber lasers," *Phys. Rev. A - At. Mol. Opt. Phys.*, vol. 77, no. 023814, pp. 1–4, 2008.

[31] E. Ding, W. H. Renninger, F. W. Wise, P. Grelu, E. Shlizerman, and J. N. Kutz, “High-energy passive mode-locking of fiber lasers,” *Int. J. Opt.*, vol. 2012, 2012.

[32] X. Liu, “Dissipative soliton evolution in ultra-large normal-cavity-dispersion fiber lasers,” *Opt. Express*, vol. 17, no. 12, p. 9549, 2009.

[33] W. J. Tomlinson, R. H. Stolen, and A. M. Johnson, “Optical wave breaking in nonlinear optical fibers,” *Opt. Lett.*, vol. 10, no. 9, pp. 457–459, 1985.

[34] Z. Wang, K. Nithyanandan, A. Coillet, P. Tchofo-Dinda, and P. Grelu, “Buildup of incoherent dissipative solitons in ultrafast fiber lasers,” vol. 2, no. 013101, pp. 1–7, 2020.

[35] R. Gumenyuk, D. A. Korobko, I. O. Zolotovsky, and O. G. Okhotnikov, “Role of cavity dispersion on soliton grouping in a fiber lasers,” *Opt. Express*, vol. 22, no. 1, p. 1896, 2014.

[36] J. R. Taylor, *Optical Solitons: Theory and Experiment*, Revised ed. Cambridge University Press, 2008.

[37] D. Y. Tang, L. M. Zhao, B. Zhao, and A. Q. Liu, “Mechanism of multisoliton formation and soliton energy quantization in passively mode-locked fiber lasers,” *Phys. Rev. A - At. Mol. Opt. Phys.*, vol. 72, no. 043816, pp. 1–9, 2005.

[38] S. M. J. Kelly, “Characteristic sideband instability of periodically amplified average soliton,” *Electron. Lett.*, vol. 28, no. 8, pp. 806–807, 1992.

[39] P. Grelu and N. Akhmediev, “Dissipative solitons for mode-locked lasers,” *Nat. Photonics*, vol. 6, pp. 84–92, 2012.

[40] Z. Wang, L. Zhan, X. Fang, and H. Luo, “Spectral filtering effect on mode-locking regimes transition: similariton-dissipative soliton fiber laser,” *J. Opt. Soc. Am. B*, vol. 34, no. 11, p. 2325, Nov. 2017.